Witten's loop in the minimal flipped $SU(5)$ unification revisited

Dylan Harries,[*] Michal Malinský,[†] and Martin Zdráhal[‡]

Institute of Particle and Nuclear Physics, Faculty of Mathematics and Physics,
Charles University in Prague, V Holešovičkách 2, 180 00 Praha 8, Czech Republic

In the simplest potentially realizable renormalizable variants of the flipped $SU(5)$ unified model the right-handed neutrino masses are conveniently generated by means of the Witten's two-loop mechanism. As a consequence, the compactness of the underlying scalar sector provides strong correlations between the low-energy flavor observables such as neutrino masses and mixing and the flavor structure of the fermionic currents governing the baryon and lepton number violating nucleon decays. In this study, the associated two-loop Feynman integrals are fully evaluated and, subsequently, are used to draw quantitative conclusions about the central observables of interest such as the proton decay branching ratios and the absolute neutrino mass scale.

I. INTRODUCTION

Though not a genuine grand unified theory (GUT), the flipped $SU(5)$ gauge theory [1–3] still attracts significant attention [4–7] due to several rather unique features it exhibits. In particular, one-stage symmetry breaking down to the standard model (SM) can be achieved regardless of whether or not a TeV-scale supersymmetry is assumed. The corresponding Higgs sector can also be very small, as it is sufficient to employ just a single 10-dimensional representation to accomplish the necessary symmetry breaking. This is to be compared to the 24 of the Georgi-Glashow $SU(5)$ [8] and/or 45 ⊕ 16 (or even 45 ⊕ 126) of the minimal $SO(10)$ GUTs (see, e.g., Refs. [9,10] and references therein).

Flipped $SU(5)$ models also share several other nice features with their truly unified cousins. From the point of view of phenomenology, two such features stand out as being particularly relevant due to their immediate experimental consequences. First, as in the $SO(10)$ GUTs, 3 right-handed (RH) neutrinos are enforced in the spectrum, allowing for the use of a type-I seesaw mechanism to generate the light neutrino masses. Additionally, as in $SU(5)$ there is only one heavy gauge boson, which typically yields somewhat stronger correlations between the flavor structure of the baryon and lepton number violating (BLNV) currents and the low-energy flavor

observables, and hence one can often say quite a bit about, e.g., the proton lifetime.

However, upon closer inspection one finds a certain level of tension between the practical implications of these two points. For example, in order to implement the standard type-I seesaw with the RH neutrinos at hand, a 50-dimensional four-index scalar 50_S of $SU(5)$ is typically added [11] together with a 3×3 complex symmetric Yukawa matrix Y_{50} in order to generate the desired RH Majorana mass term via a renormalizable coupling such as $Y_{50}^{IJ} 10_{FI}^T C^{-1} 10_{FJ} 50_S$. Besides enlarging the scalar sector enormously (and, hence, disposing of the uniquely small size of the "minimal" Higgs sector noted above as one of the most attractive structural features of the framework), the extra scalar and the associated Yukawa at play reduces the value of the low-energy neutrino masses and the lepton mixing data as constraints for the proton lifetime estimates as it essentially leaves the neutrino sector on its own.

Remarkably enough, this dichotomy may be overcome by noticing [12,13] that the RH neutrino masses in flipped $SU(5)$ models may be generated even without the unpleasant extra 50_S at the two-loop level by means of a variant of the mechanism first identified by Witten in the $SO(10)$ context [14]. The two main features [13] of this scenario are, first, a simple relation among the seesaw and the GUT scales where the former is, roughly speaking, given by the latter times an extra two-loop suppression and, second, a rigid correlation between the flavor structures of the neutrino and charged sectors, which in most cases may be transformed into a set of strong constraints for, e.g., the proton decay partial widths and branching ratios.

To this end, the Witten's-loop-equipped flipped $SU(5)$ may even be viewed as *the most economical renormalizable theory of the BLNV nucleon decays*, much simpler

[*]harries@ipnp.troja.mff.cuni.cz
[†]malinsky@ipnp.troja.mff.cuni.cz
[‡]zdrahal@ipnp.troja.mff.cuni.cz

than, e.g., the potentially realistic variants of the $SO(10)$ and even the $SU(5)$ GUTs.

From this perspective, it is interesting that in Ref. [13] most of the basic features of this framework may have been identified even without an explicit calculation of the graphs involved in Witten's mechanism. In this work we intend to overcome this drawback by a careful inspection of the Feynman graphs and their evaluation which, as we shall see, will clarify several other points left unaddressed in the preceding studies. In particular, the calculation will make it very clear that the minimal potentially realistic and renormalizable incarnation of the scheme under consideration is the variant featuring a pair of 5-dimensional scalars in the Higgs sector (besides a single copy of the "obligatory" 10-dimensional 10_H scalar). Second, it will be shown that, in this framework, the light neutrino spectrum is always forced to be on the heavy side (actually, within the reach of the KATRIN experiment [15]), which, among other things, provides a clear smoking gun signal of the scheme.

In Sec. II we first provide a brief review of the flipped $SU(5)$ gauge theory context, identify the Feynman graphs underpinning the radiative RH neutrino mass generation in the minimal and next-to-minimal models, and exploit the seesaw formula in order to get strong constraints on their parameter space. Section III is devoted to a detailed analysis of the relevant two-loop graphs in the scenario with one copy of the 5-dimensional scalar in the Higgs sector; this setting is simple enough to allow for a complete analytic understanding of the results. In Sec. IV these findings are used for the identification of the minimal potentially realistic model of this kind, which is subsequently shown to be strongly constrained and potentially highly predictive. Most of the technical details of the lengthy calculations are deferred to a set of Appendices.

II. FLIPPED $SU(5)$ À LA WITTEN

The defining feature of the flipped $SU(5)$ unifications is the "nonstandard" embedding of the SM hypercharge operator within its $SU(5) \otimes U(1)_X$ gauge symmetry algebra, namely

$$Y = \frac{1}{5}(X - T_{24}), \qquad (1)$$

where T_{24} stands for the usual hypercharge-like generator of the standard $SU(5)$ (normalized in such a way that the electric charge obeys $Q = T_L^3 + T_{24}$) and X is the unique nontrivial anomaly-free generator of the additional $U(1)$ normalized in such a way that it receives integer values over the three basic irreps accommodating each generation of the SM matter,

$$\bar{5}_M \equiv (\bar{5}, -3), \qquad 10_M \equiv (10, +1), \qquad 1_M \equiv (1, +5),$$
$$(2)$$

where the first number in brackets gives the $SU(5)$ representation and the second the charge under $U(1)_X$. Compared to the standard $SU(5)$ case, the SM matter fields u_L^c and d_L^c are swapped with respect to their usual assignments, i.e., the former is a member of $\bar{5}_M$ while the latter resides in 10_M. Similarly, e_L^c is found in the $SU(5)$ singlet and the compulsory RH neutrino ν_L^c replaces it in the 10-plet.

As for the gauge fields, the $(24, 0) \oplus (1, 0)$ adjoint of $SU(5) \otimes U(1)_X$ in this context contains a multiplet X_μ transforming under $SU(3)_C \otimes SU(2)_L \otimes U(1)_Y$ as $(3, \bar{2}, +\frac{1}{6})$, plus its Hermitian conjugate, rather than the traditional hypercharge-$\frac{5}{6}$ gauge bosons of the standard $SU(5)$. The remaining degrees of freedom account for the 12 SM gauge fields and one additional heavy singlet.

The minimal Higgs sector sufficient for breaking the $SU(5) \otimes U(1)$ symmetry down to the SM and, subsequently, to the $SU(3) \otimes U(1)$ of QCD + QED consists of $10_H = (10, +1)$,[1] in which the SM singlet occupies the same position as the RH neutrino does in 10_M, and $5_H = (5, -2)$ containing the SM Higgs doublet. The breakdown of $SU(5) \otimes U(1)_X$ to the SM gauge symmetry takes place after the SM singlet present in 10_H develops a non-zero vacuum expectation value (VEV), V_G, generating masses

$$m_X^2 = \frac{g_5^2 V_G^2}{2} \qquad (3)$$

for the gauge bosons X_μ, where g_5 is the $SU(5)$ gauge coupling. The color triplet, $SU(2)_L$ singlet components of 10_H and 5_H also mix at this stage to form a pair of massive color triplets $\Delta_{1,2}$ transforming under the SM gauge symmetry as $(3, 1, -\frac{1}{3})$, with masses $m_{\Delta_{1,2}}$. Further details regarding the tree-level scalar spectrum in this minimal flipped $SU(5)$ model are given in Appendix B.

For the above embedding of the SM matter content and minimal set of Higgs scalars, one can readily write the most general renormalizable[2] Yukawa Lagrangian (suppressing all flavor indices)

---

[1]It may be worth pointing out here that, due to the nonzero $U(1)_X$ charge of 10_H inherent to the flipped $SU(5)$ models, there is no way to build a nonrenormalizable $d = 5$ operator (presumably Planck-scale suppressed) that might, in the broken phase, affect the gauge-kinetic form and hence introduce significant theoretical uncertainties in the high-scale gauge-matching conditions and the determination of the GUT scale. As a result, one of the primary sources of irreducible uncertainties hindering the predictive power of the "standard" GUTs (such as the Georgi-Glashow $SU(5)$ or the nonminimal $SO(10)$ models with either 54 or 210 breaking the unified symmetry) is absent from this class of models.

[2]Note that in nonrenormalizable settings the benefits of the scheme may be lost as the Witten's loop contribution may be swamped by the effects of, e.g., the $d = 5$ nonrenormalizable operators of the $10_M 10_M 10_H 10_H$ type.

$$\mathcal{L} \ni Y_{10} 10_M 10_M 5_H + Y_{\bar{5}} 10_M \bar{5}_M 5_H^* + Y_1 \bar{5}_M 1_M 5_H + \text{H.c.},$$

$$(4)$$

with Y_{10}, $Y_{\bar{5}}$, and Y_1 denoting the relevant 3×3 complex Yukawa coupling matrices; note that the first of these, unlike the latter two, is required to be symmetric in its flavor indices, i.e., $Y_{10} = Y_{10}^T$. In the broken phase, the second term in Eq. (4) yields a strong correlation among the Dirac neutrino mass matrix M_ν^D and the up-type quark mass matrix M_u, namely,

$$M_\nu^D = M_u^T \qquad (5)$$

at the GUT scale. The flavor symmetric nature of Y_{10} also means that the down-type quark mass matrix satisfies $M_d = M_d^T$, while the couplings in Eq. (4) say nothing specific about the mass matrix M_e of the charged leptons. As we shall see, these correlations will turn out to be central for the high degree of predictivity of this framework[3] entertained in the following sections.

A. The RH neutrino masses and type-I seesaw

So far, we have left aside any discussion of the physical light neutrino masses in the current scenario. Obviously, Eq. (5) cannot be the whole story as it corresponds to overly large Dirac neutrino masses; the only case when this may be acceptable would be within a variant of the seesaw mechanism.

At the tree level, this could be achieved in the most natural way by employing a 50-dimensional scalar [11] coupled to the $10_M^T C^{-1} 10_M$ fermionic bilinear; the VEV of a singlet therein then gives rise to the desired RH neutrino mass term. However, as was noted in Sec. I, the associated single-purpose extra Yukawa matrix does not bring any additional insight into the flavor structure of the model, and limits the extent to which low-energy data can be used in constraining proton decay observables. Therefore we do not adopt this option here; instead, we inspect the quantum structure of the minimal model for the desired effect.

Remarkably enough, there is no way to generate the desired RH neutrino mass in the current model [13] at the one-loop level. This, however, does not mean that there is no one-loop contribution to the neutrino masses generated at all; indeed, in the presence of scalars with quantum numbers $(3, 1, -\frac{1}{3})$ and $(3, \bar{2}, +\frac{1}{6})$ the LH Majorana mass can be devised via a "colored" variant of the notorious Zee mechanism [16–19]. However, this does not bring any relief to the Dirac mass issue above as, without additional

---

[3]To this end, it is worth noting that these relations remain intact even in models with more than a single copy of 5_H in the scalar sector; as we shall see, this (especially the symmetry of M_d) will be crucial for the construction of the minimal potentially realistic scenario identified in Sec. IV B.
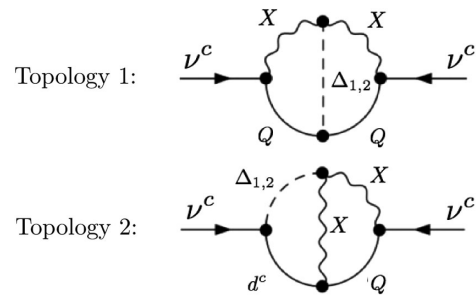

FIG. 1. The two nonequivalent topologies of the two-loop graphs contributing to the RH neutrino Majorana mass in the minimal flipped $SU(5)$ model under consideration. The vector field X corresponds to the $(3, \bar{2}, +\frac{1}{6})$ component of the adjoint while the pair of Δ's are the two mass eigenstates of the $(3, 1, -\frac{1}{3})$ colored scalars mixed from the relevant components of 10_H and 5_H, respectively.

structure, one is still left with GeV-scale neutrinos, albeit pseudo-Dirac instead of Dirac in nature.

1. The Witten's loop structure

The simultaneous presence of the diquark-type of interactions, mediated by the X_μ and $\Delta_{1,2}$ bosons, together with their leptoquark counterparts (involving the same set of fields) in the flipped $SU(5)$ framework implies that diagrams generating the desired RH Majorana neutrino mass can be drawn at two loops. Let us note that the corresponding pair of topologies depicted in Fig. 1 can be viewed as reduced versions of Witten's original $SO(10)$ graph(s) [14].

In what follows we shall work in the broken phase perturbation theory with masses in the free Hamiltonian[4] and in the unitary gauge so that there are no Goldstone modes around. This reduces the number of relevant graphs considerably, at the cost of making the Feynman integrals somewhat more complicated compared to other cases.

Based on the graphs in Fig. 1 that remain in this approach, it is immediately possible to make several comments on both the flavor structure and overall scale of the generated Majorana mass matrix M_ν^M. The flavor structure in particular plays a central role in what follows, and is governed by the Yukawa couplings appearing in each of the contributing graphs. In each of the two topologies there is only a single Yukawa coupling present, associated with the couplings of Δ_i to the fermions. These couplings involve only the 5_H components of Δ_i, since it is only these

---

[4]Hence, we are avoiding the need to sum over an infinite tower of graphs (like the one drawn in Witten's original work [14]) with increasing numbers of VEV insertions. On the other hand, the explicit proportionality to the μ parameter governing the mixing between the 10_H and 5_H multiplets (see Appendix B), which is obvious in the massless perturbation theory, becomes more involved in the massive case where μ emerges at the level of the relevant mixing matrix in the scalar sector, Eq. (B8).

components that couple to the fermions through the Yukawa interactions in Eq. (4). Moreover, since all of the fermions appearing in the two graphs in Fig. 1 reside in 10_M, the single relevant Yukawa coupling matrix is the symmetric Y_{10}. Hence, in the minimal model there is a tight correlation between the radiatively generated RH neutrino Majorana mass matrix and the mass matrix of the down-type quarks, making the scheme rather predictive.

The overall scale of M_ν^M, on the other hand, depends on both the Yukawa couplings in Y_{10} as well as the gauge couplings and the sizes of the mass parameters entering into each of the graphs. One can initially estimate it to be proportional to the dominant mass entry in the relevant graphs suppressed by the appropriate two-loop factor and the combination of gauge (entering raised to the fourth power) and Yukawa couplings.

Of the various mass parameters appearing in the evaluation of the graphs, the fermionic masses m_f should play no role in the integrals as the singlet Majorana mass generation does not rely on the electroweak symmetry breaking. Hence, in dealing with the Feynman integration we shall work in the chiral limit with all SM fermions massless. This, in principle, may lead to spurious IR divergences in the form of, e.g., $\log(m_f/Q)$ arising in individual partial fractions of the integrands, where Q is the renormalization scale, but as a whole M_ν^M should be stable in the $m_f \to 0$ limit.

Similarly, it is natural to expect that in the other extreme case corresponding to one of the scalars Δ_i becoming significantly lighter with respect to the X_μ boson masses (and, hence, bringing about another practically massless propagator) M_ν^M should also remain regular; hence, the only mass that can make it to the denominators in the final result is m_X. This also suggests that, barring the couplings, each individual graph should be governed by powers of the m_{Δ_i}/m_X ratio which, in turn, makes it merely a function of a single[5] parameter.

One more comment concerning the relative size of the aforementioned one-loop LH Majorana neutrino mass contribution is worth making here. On purely dimensional grounds, it is indeed expected to be significantly smaller than the "standard" type-I contribution due to M_ν^M and M_ν^D. First, the corresponding graphs will be inversely proportional to the relevant scalar leptoquark masses,[6] which are well above the typical seesaw scale ballpark of 10^{12-13} GeV. Second, the loop factor of $1/16\pi^2$ will

further suppress this contribution placing it, eventually, at the level of some 10^{-6} eV, which makes it negligible for the current analysis.

2. Seesaw as the key to the phenomenology

Before coming to the evaluation of the graphs in Fig. 1 it is important to stress that this is not all just an academic exercise; quite to the contrary, the information obtained in Sec. III has a profound impact on the phenomenology of the model.

The point is that, due to the seesaw formula, M_ν^M is correlated with the physical light neutrino mass matrix m_{LL} and the Dirac neutrino mass matrix M_ν^D via

$$M_\nu^D (m_{LL})^{-1} (M_\nu^D)^T = -M_\nu^M. \tag{6}$$

Using Eq. (5), this can be conveniently written as

$$W_\nu \equiv D_u U_\nu^\dagger (m_\nu^{\text{diag}})^{-1} U_\nu^* D_u = -M_\nu^M, \tag{7}$$

where D_u is the diagonal form of the up-type quark mass matrix and U_ν is the matrix diagonalizing m_{LL}, i.e., $m_{LL} = U_\nu^T m_\nu^{\text{diag}} U_\nu$. Note that in the derivation above we have implicitly adopted the basis in which the up-type quark mass matrix is real and diagonal, see Ref. [13] for further information.

Hence, up to an *a priori* unknown unitary matrix and the overall light neutrino mass scale, parametrized e.g., by the mass of the heaviest of the light neutrinos $m_\nu^{\max}$, the matrix W_ν defined in Eq. (7) is completely determined by the low-energy quark masses and neutrino oscillation data. This is to be compared with M_ν^M appearing as the right-hand side of Eq. (7), which is set by the heavy spectrum of the model (i.e., the masses of the heavy triplet scalars and gauge bosons) and the gauge and Yukawa couplings, and is therefore subject to other strong constraints. In particular, m_X, m_{Δ_i} and g_5 must be such that the unification pattern is consistent with the low-energy data and compatible with the nonobservation of proton decay with at least 10^{34} years of lifetime [20].

Hence, demanding consistency of Eq. (7) with the data one can derive constraints on $m_\nu^{\max}$ and, in particular, on U_ν, which is central to the BLNV phenomenology of the model. Indeed, U_ν drives all the proton decay branching ratios into neutral mesons including the "golden channel" $p \to \pi^0 e^+$ final state:

$$\frac{\Gamma(p \to \pi^0 e_\alpha^+)}{\Gamma(p \to \pi^+ \bar\nu)} = \frac{1}{2} |(V_{\text{CKM}})_{11}|^2 |(V_{\text{PMNS}} U_\nu)_{\alpha 1}|^2,$$

$$\frac{\Gamma(p \to \eta e_\alpha^+)}{\Gamma(p \to \pi^+ \bar\nu)} = \frac{C_2}{C_1} |(V_{\text{CKM}})_{11}|^2 |(V_{\text{PMNS}} U_\nu)_{\alpha 1}|^2,$$

$$\frac{\Gamma(p \to K^0 e_\alpha^+)}{\Gamma(p \to \pi^+ \bar\nu)} = \frac{C_3}{C_1} |(V_{\text{CKM}})_{12}|^2 |(V_{\text{PMNS}} U_\nu)_{\alpha 1}|^2, \tag{8}$$

---

[5]Assuming, implicitly, that the renormalization scale dependence eventually disappears as a consequence of the assumed UV-finiteness of the full result.

[6]It is perhaps worth mentioning that the scalar (S) with the SM quantum numbers $(3, \bar{2}, +\frac{1}{6})$ is formally absent in the unitary gauge as it is the would-be Goldstone mode giving mass to the X^μ vector; however, the same effect is then generated via the corresponding graphs with X^μ instead of S.

where the C_i's are various low-energy factors calculable using chiral Lagrangian techniques (see, e.g., Ref. [21] and references therein) and V_{CKM} and V_{PMNS} are the Cabibbo-Kobayashi-Maskawa and the Pontecorvo-Maki-Nakagawa-Sakata mixing matrices, respectively.

In this sense, the minimal flipped $SU(5)$ unification equipped with the Witten's loop mechanism can be viewed as a particularly simple (if not the most minimal of all) theory of the absolute neutrino mass scale and, at the same time, the two-body BLNV nucleon decays.

B. Consistency constraints and implications

Let us now work out the aforementioned consistency constraints in more detail and give some basic examples of their possible implications. First, it should be noted that there is a lower limit on the largest entry of W_ν that depends on m_ν^{max} and the shape of U_ν. Taking into account the typical 50% reduction of the running top quark Yukawa between M_Z and the unification scale (at around 10^{16} GeV) and taking, e.g., $m_\nu^{\text{max}} = 1$ eV and $U_\nu = 1$ one finds that the (3,3) entry of W_ν is as large as about

$$|(W_\nu)_{33}| \sim 6.4 \times 10^{12} \text{ GeV}. \qquad (9)$$

The same magnitude, however, may not so easily be achieved for the (3,3) entry of M_ν^M as required by Eq. (7) due to the generic 10^{-3} geometrical suppression in the relevant two-loop graphs and a possible further suppression associated with the Yukawa coupling Y_{10}; the latter may be especially problematic in the minimal scenario (4) because then Y_{10} is fixed by the down-type quark masses and, thus, brings about another suppression of some 10^{-2} to $(M_\nu^M)_{33}$.

However, this correlation is loosened if there is more than a single copy of 5_H in the scalar sector. As was already indicated in Ref. [13], the additional Y'_{10} associated to an extra $5'_H$ can conspire with the original Y_{10} to do two things at once: they may partially cancel in the down-type quark mass formula to account for the moderate suppression of M_d/M_Z yet their other combination governing M_ν^M (weighted by the appropriate scalar mixings) may still remain large, thus avoiding the problematic additional 10^{-2} suppression. In what follows, we shall model this situation by imposing a humble $|y| \lesssim 4\pi$ perturbativity criterion on all the Y_{10} and Y'_{10} entries.

However, even in such a case the $\sim 10^{13}$ GeV lower limit on the largest entry $(W_\nu)_{33}$, may still be problematic because, for $U_\nu \neq 1$, it may be further enhanced by the admixture of the yet larger (2,2) and, in particular, the (1,1) entry of $(m_\nu^{\text{diag}})^{-1}$; as a matter of fact the latter is not constrained at all given that the lightest neutrino mass eigenstate may still be extremely light. Thus, the lower bound on the magnitude of the largest element of W_ν gets further boosted over the naïve estimate of 10^{13} GeV

whenever U_ν departs significantly from unity, which in turn constrains all of the partial widths, Eqs. (8).

Hence, a thorough evaluation of the graphs in Fig. 1 will decide several important questions, namely:

(1) Can the elements of M_ν^M ever be big enough to be consistent (at least in the most optimistic scenario with $U_\nu \sim 1$) with W_ν, as required by Eq. (7), in the case of the single 5_H scenario with its typical extra 10^{-2} suppression at play?

(2) If not, can the two-5_H scenario work? What would be then the corresponding lower limit for m_ν^{max} in this scenario?

(3) In either case, what is the allowed domain for the entries of U_ν and, thus, for the corresponding BLNV nucleon decay rates?

This is what we turn our attention to in the remainder of this article.

III. WITTEN'S LOOP CALCULATION

The leading contribution to the radiatively generated RH neutrino mass in the current scheme may be computed by considering the graphs in Fig. 1 evaluated at zero external momentum, see Appendix C, with the relevant interaction terms given in Appendix A. In the minimal renormalizable model containing only a single 10_H and one or more 5_H representations, no one-loop contribution to the RH neutrino mass matrix can be generated, nor do there exist any one-loop counterterm graphs. The resulting expression for the RH Majorana neutrino mass matrix in the case of a single 5_H multiplet reads

$$(M_\nu^M)^{IJ} = -\frac{3g_5^4}{(4\pi)^4} V_G \sum_{i=1}^{2} (-8Y_{10}^{IJ})(U_\Delta)_{i1}(U_\Delta^*)_{i2} I_3(s_i), \qquad (10)$$

where the scalar mixing matrix elements $(U_\Delta)_{ij}$ are given in Appendix B, and $I_3(s_i)$ is the sum of the corresponding loop integrals evaluated at zero external incoming momentum,

$$I_3(s_i) = -(4\pi)^4 (\Sigma_1^P(0) + 2\Sigma_2^P(0)), \qquad (11)$$

regarded as a function of $s_i = m_{\Delta_i}^2/m_X^2$. Recall that there is an overall extra factor of 2 included in Eq. (10) related to the permutation of the two external neutral field lines (for $I = J$) or to the symmetry of Y_{10} (for $I \neq J$). The integrals $\Sigma_1^P(0)$ and $\Sigma_2^P(0)$, corresponding to topology 1 and 2 respectively, are given by

$$i\Sigma_1^P(0) = i \int \frac{d^4p}{(2\pi)^4} \int \frac{d^4q}{(2\pi)^4} \gamma_\rho \frac{1}{-\slashed{q}} \frac{1}{\slashed{p}} \gamma_\mu$$

$$\times \frac{1}{(p+q)^2 - m_{\Delta_i}^2} \frac{-g^{\mu\nu} + \frac{1}{m_X^2}p^\mu p^\nu}{p^2 - m_X^2} \frac{-g_\nu^\rho + \frac{1}{m_X^2}q_\nu q^\rho}{q^2 - m_X^2}, \qquad (12)$$

$$i\Sigma_2^P(0) = i \int \frac{d^4p}{(2\pi)^4} \int \frac{d^4q}{(2\pi)^4} \frac{1}{-\not q}\gamma_\rho \frac{1}{\not p}\gamma_\mu \frac{1}{q^2 - m_{\Delta_i}^2}$$

$$\times \frac{-g^{\mu\nu} + \frac{1}{m_X^2}p^\mu p^\nu}{p^2 - m_X^2} \frac{-g_\nu^\rho + \frac{1}{m_X^2}(p+q)_\nu(p+q)^\rho}{(p+q)^2 - m_X^2}.$$

$$(13)$$

The integrals in Eqs. (12) and (13) are evaluated by reducing them to expressions involving (variants of) the brackets by Veltman and van der Bij [22], which may be evaluated directly [22–27]. The details of this reduction, and the resulting analytic expressions for the two-loop integrals, are given in Appendix D. In particular, using the results given in Ref. [22] and appropriate generalizations thereof, it is found that the contributing brackets are free of potential IR divergences in the limit of massless internal fermions, such that the fermion masses may safely be allowed to vanish as in Eqs. (12) and (13). On the other hand, each graph is individually UV divergent. Setting $\epsilon = 2 - \frac{D}{2}$, where D is the spacetime dimensionality, the divergences are found to be

$$-(4\pi)^4\Sigma_1^{P,\text{div}}(0) = \frac{3}{2\epsilon} - \frac{m_{\Delta_i}^4}{2m_X^4}\left(\frac{1}{2\epsilon^2} + \frac{3}{2\epsilon} - \frac{1}{\epsilon}\log\frac{m_{\Delta_i}^2}{Q^2}\right),$$

$$(14)$$

and

$$-(4\pi)^4\Sigma_2^{P,\text{div}}(0) = -\frac{3}{4\epsilon} + \frac{m_{\Delta_i}^4}{4m_X^4}\left(\frac{1}{2\epsilon^2} + \frac{3}{2\epsilon} - \frac{1}{\epsilon}\log\frac{m_{\Delta_i}^2}{Q^2}\right).$$

$$(15)$$

It follows from Eq. (11) that the total contribution $I_3(s_i)$ to the RH neutrino mass matrix is UV finite, as must be the case here due to the absence of the necessary counterterms.

IV. RESULTS

The behavior of the result for the purely kinematic piece of the RH neutrino mass matrix, $I_3(s)$, is shown in Fig. 2. Notably, the magnitude of $I_3(s)$ is bounded for all $s \geq 0$. Indeed, from the analytic result given in Eq. (D31), one has that for $s \to 0$,

$$I_3(s \to 0) = 3 + s\left(3\log s + \pi^2 - \frac{15}{2}\right) + O(s^2\log^2 s),$$

$$(16)$$

while in the opposite limit with $s \to \infty$,

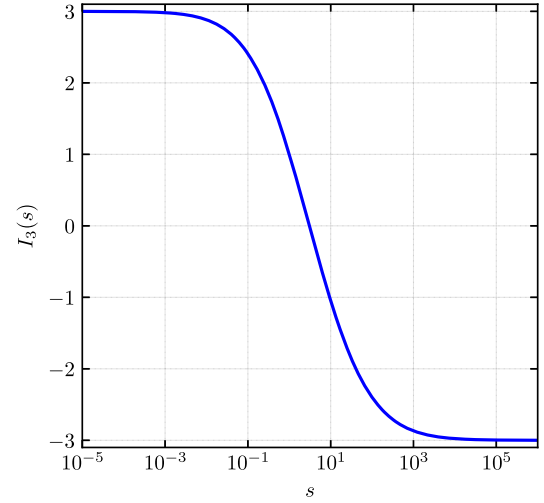$$I_3(s \to \infty) = -3 + O(s^{-1}\log^2 s). \qquad (17)$$

FIG. 2. Plot of the function $I_3(s)$ appearing in the RH neutrino mass matrix.

A. RH neutrino masses in the minimal model

With $I_3(s)$ determined, we may proceed to evaluate the size of M_ν^M in Eq. (10). Substituting in the explicit forms of the mixing matrix elements in Eq. (B11) one obtains

$$M_\nu^M = -\frac{3g_5^4}{(4\pi)^4}(-8Y_{10})V_G\tilde{I}, \qquad (18)$$

where

$$\tilde{I} = \sum_{i=1}^2 \frac{2\nu^*(2\lambda_2 + g_5^2 s_i)}{4|\nu|^2 + (2\lambda_2 + g_5^2 s_i)^2}I_3(s_i), \qquad (19)$$

and $\nu = \mu/V_G$. We note that $\tilde{I} \to 0$ as $\mu \to 0$, reflecting the fact that the graphs rely on the $10_H - 5_H$ mixing. It is also clear from Eq. (19) that, since $I_3(s)$ is bounded, $\tilde{I}$ cannot be made arbitrarily large to compensate for the suppression factors noted in Sec. II. To develop some sense of the allowed size of $\tilde{I}$, it is useful to substitute for s_i from Eq. (B7) and inspect $\tilde{I}$ as a function of ν, λ_2, λ_5, and g_5, neglecting all terms that are of the order of v^2/V_G^2, where v is the electroweak VEV, see Eq. (B2). Requiring that the tree-level vacuum be locally stable implies [13] $\lambda_{2,5} < 0$ and

$$|\nu| \leq \sqrt{\lambda_2\lambda_5}. \qquad (20)$$

When this bound is saturated, i.e., when $|\nu| = \sqrt{\lambda_2\lambda_5}$, the mass m_{Δ_1} vanishes for all values of λ_2, λ_5 while $m_{\Delta_2}^2 = -(\lambda_2 + \lambda_5)V_G^2$. The resulting value of $\tilde{I}$ for this special case is shown in the (λ_2, λ_5) plane in Fig. 3. In particular, it should be noted that the value of $\tilde{I}$ is unchanged under the interchange $\lambda_2 \leftrightarrow \lambda_5$, as can be easily verified from Eqs. (19) and (B7), and $|\tilde{I}| \leq 3$ for all values of λ_2 and λ_5. The maximal value of $|\tilde{I}|$ is achieved for $\lambda_2 = \lambda_5$, with $|\tilde{I}| \to 3$ as $\lambda_2 = \lambda_5 \to -\infty$.
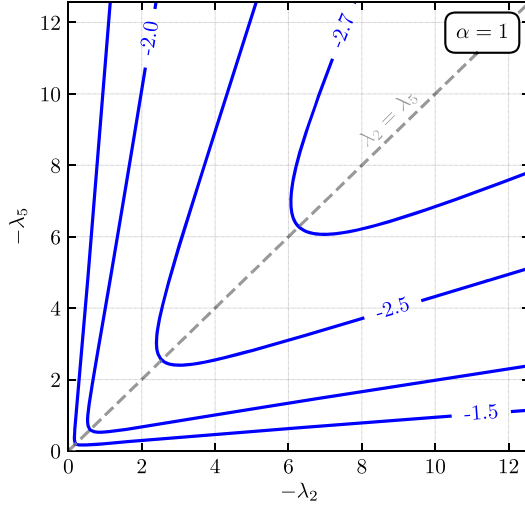
FIG. 3.   Contour plot of $\tilde{I}$, as defined in Eq. (19), in the (λ_2, λ_5)-plane, with $g_5 = 0.5$ and $\nu = \alpha\sqrt{\lambda_2\lambda_5}$ for $\alpha = 1$, corresponding to the maximal value of $|\nu|$ consistent with a locally stable SM vacuum.

Qualitatively different behavior results in the more general case that ν does not saturate the bound given in Eq. (20). This is demonstrated in Fig. 4, in which the value of $\tilde{I}$ is plotted as a function of $\lambda_2 = \lambda_5 = \lambda$ with

$$\nu = \alpha\sqrt{\lambda_2\lambda_5}, \qquad \alpha \in [0, 1], \qquad (21)$$

for several values of α. Although $\tilde{I}$ remains invariant under $\lambda_2 \leftrightarrow \lambda_5$, with the maximum value of $|\tilde{I}|$ still occurring for $\lambda_2 = \lambda_5$, for values of $|\alpha| < 1$, $|\tilde{I}|$ now tends to zero for large values of the scalar couplings λ_2, λ_5. This is due to the fact that, for $|\alpha| \neq 1$, both s_1, s_2 grow with increasing $|\lambda|$ such that $I_3(s_1), I_3(s_2) \to -3$, while the coefficients of
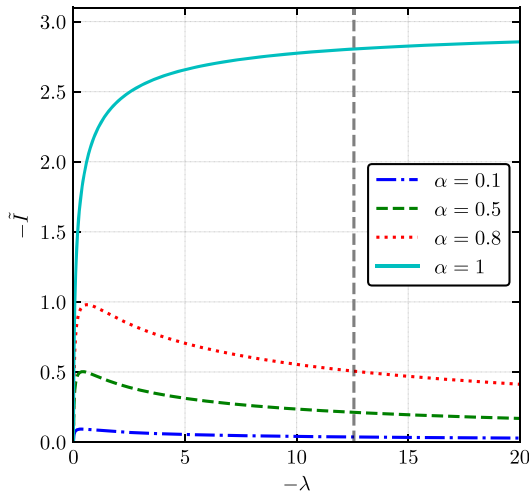

FIG. 4.   Plot of the range of variation of $\tilde{I}$ as a function of $\lambda_2 = \lambda_5 = \lambda$, with $g_5 = 0.5$ and $\mu = \alpha\sqrt{\lambda_2\lambda_5}V_G$, for $\alpha \in [0, 1]$. The dashed vertical line denotes the naïve perturbativity limit $|\lambda_i| \leq 4\pi$.

each in Eq. (19) are equal in magnitude but of opposite sign, resulting in the two terms cancelling. Physically, this corresponds to the expected dynamical decoupling of the heavy scalar states in the $m_{\Delta_{1,2}} \to \infty$ limit. For $\alpha = 1$, at least one color triplet scalar is massless at tree-level for all values of λ_2 and λ_5. Consequently, this state never decouples and $\tilde{I}$ therefore does not vanish. Technically, this arises because $I_3(s_1) = 3$ while $I_3(s_2) \to -3$, with the two contributions still entering $\tilde{I}$ with coefficients of equal magnitude but opposite sign.

However, even in the most optimistic case with $|\tilde{I}| \to 3$, the above results make it clear that there is little hope for a viable prediction of the light neutrino spectrum in the minimal scenario under consideration. For acceptable values of $m_X \sim 10^{17}$ GeV, and taking $g_5 \approx 0.5$, the elements of M_ν^M are found to be $\lesssim 10^{12}$ GeV after taking into account $\sim 10^{-2}$ suppression associated with presence of Y_{10}. This is to be compared with the (optimistic) lower bound of $\sim 10^{13}$ GeV for the elements of the left-hand side of Eq. (7). Evidently, in the case when only a single 5_H is present in the spectrum the answer to whether Eq. (7) can be satisfied is negative. In fact, in this minimal model the problem is exacerbated by the fact that $Y_{10} \propto M_d$, which implies a far too hierarchical pattern of light neutrino masses irrespective of their absolute size, as was previously noted in Ref. [13]. Thus we are immediately led to consider the remaining questions raised in Sec. II concerning the viability of the model with an additional 5_H representation instead.

B. Minimal potentially realistic model

As noted above, the addition of a second 5_H multiplet in principle allows both the Y_{10} suppression and the overly hierarchical flavor structure to be avoided. At the same time, the overall predictive power of the theory is not significantly harmed by this addition; in particular, doing so does not spoil the key Yukawa relations used in obtaining Eq. (7). With a second $5_H'$ multiplet, the Yukawa sector of the model reads

$$\begin{aligned}
\mathcal{L} \ni\ & Y_{10}10_M10_M5_H + Y_{10}'10_M10_M5_H' \\
& + Y_{\bar{5}}10_M\bar{5}_M5_H^* + Y_{\bar{5}}'10_M\bar{5}_M5_H'^* \\
& + Y_1\bar{5}_M1_M5_H + Y_1'\bar{5}_M1_M5_H' + \text{H.c.}, \quad (22)
\end{aligned}$$

where Y_{10}' is of course also flavor symmetric. In this scenario, the Dirac neutrino mass matrix still remains tightly correlated with the up-type quark masses, with the GUT scale relation

$$M_\nu^D = M_u^T \propto Y_{\bar{5}}v + Y_{\bar{5}}'v' \qquad (23)$$

holding at tree-level, where v' is the VEV associated with the electrically neutral component of $5_H'$, see Appendix B 2. By contrast, the analogous relationship between the

down-type quark masses and the generated RH neutrino Majorana masses, M_d, $M_\nu^M \propto Y_{10}$, is no longer preserved. While $M_d \propto Y_{10}v + Y'_{10}v'$, the appropriate generalization of Eq. (10) reads

$$(M_\nu^M)^{IJ} = -\frac{3g_5^4}{(4\pi)^4} V_G \sum_{i=1}^3 \sum_{j=2}^3 (-8Y_j^{IJ})(U_\Delta)_{i1}(U_\Delta^*)_{ij} I_3(s_i), \tag{24}$$

where $Y_j = Y_{10}$ when $j = 2$ and $Y_j = Y'_{10}$ when $j = 3$, with U_Δ now a 3×3 mixing matrix as defined in Eq. (B16). Thus, in general, M_d and M_ν^M are determined by different linear combinations of the Yukawa couplings Y_{10} and Y'_{10}. In turn, this means that the generic suppression of M_ν^M by a factor $\propto M_d$ may be avoided in the two-5_H scenario. On the other hand, it is still the case that the elements of M_ν^M are bounded from above, at least so long as it is required that all couplings remain perturbative.

1. Phenomenology of the minimal potentially realistic model

As the ignorance of yet higher-order effects makes any such perturbativity constraints somewhat arbitrary in general, in what follows we shall give two examples of the M_ν^M estimates corresponding to two different choices of the upper limits on the effective (running) SM down-quark Yukawa couplings. These, according to Eq. (A3), obey $Y_d \equiv 8Y_{10}$ and $Y'_d \equiv 8Y'_{10}$ at the matching scale. The two cases to be considered are (i) $|Y_d|$, $|Y'_d| \lesssim 1$ and (ii) $|Y_d|$, $|Y'_d| \lesssim 4\pi$. For the former case (motivated by the SM value of the top Yukawa coupling) one has the following upper limit on M_ν^M calculated from Eq. (24)

$$\text{case i) } |M_\nu^M| \lesssim 6.4 \times 10^{12} \left(\frac{m_X}{10^{17}\text{ GeV}}\right) \text{ GeV}, \tag{25}$$

while for the latter one obtains

$$\text{case ii) } |M_\nu^M| \lesssim 8.0 \times 10^{13} \left(\frac{m_X}{10^{17}\text{ GeV}}\right) \text{ GeV}. \tag{26}$$

Note that in both cases we have used the (numerical) upper limit

$$\left| \sum_{i=1}^3 \sum_{j=2}^3 (U_\Delta)_{i1}(U_\Delta^*)_{ij} I_3(s_i) \right| \leq 3 \tag{27}$$

which is completely analogous to the limit discussed in Sec. IV A for the single-5_H case.

Remarkably, for the typical flipped $SU(5)$ value of $m_X = 10^{17}$ GeV (see, e.g., Ref. [13]) the case (i) limit, Eq. (25), is just on the borderline of compatibility with the optimistic

lower limit in Eq. (9) on $|W_\nu|$, while the latter case (ii) in principle admits lower[7] values of m_X.

This, in turn, implies that there is generally not much room for any significant admixture of the second neutrino (inverse) mass within the element $(W_\nu)_{33}$, hence, the only allowed U_ν's in Eq. (7) are those for which $(U_\nu)_{13}$ and $(U_\nu)_{23}$ are small.

To this end, the model clearly calls for a dedicated numerical analysis including a detailed calculation of the heavy spectrum that conforms to, among other things, the requirement of a significant spread of the scalar triplets in order to maximize $|\tilde{I}|$. This, however, is beyond the scope of the current study and will be elaborated on elsewhere.

At this point, let us just illustrate the typical situation by evaluating the most significant proton-decay two-body branching ratios (neglecting the kinematically suppressed vector-meson channels for simplicity) in the $(U_\nu)_{13} = (U_\nu)_{23} = 0$ limit with the 1-2 mixing angle θ_{12} therein chosen in such a way that $\Gamma(p \to \pi^0\mu^+)$ is maximized (see Ref. [13] for further details):

$$\begin{aligned} \text{Br}(p \to \pi^+\bar{\nu}) &\approx 80.0\%, \\ \text{Br}(p \to \pi^0 e^+) &\approx 14.2\%, \\ \text{Br}(p \to \pi^0\mu^+) &\approx 5.5\%, \\ \text{Br}(p \to K^0 e^+) &\approx 0.1\%. \end{aligned} \tag{28}$$

Needless to say, for nonextremal values of θ_{12} these branching ratios may vary; in particular, $\text{Br}(p \to \pi^0 e^+)/\text{Br}(p \to \pi^0\mu^+)$ should increase.

Finally, let us say a few words about the lower limits on the mass of the heaviest SM neutrino in the two cases (25) and (26). As for the former, one obtains[8]

$$m_3 \gtrsim \left(\frac{10^{17}\text{ GeV}}{m_X}\right) \text{ eV} \tag{29}$$

while for the latter one has

$$m_3 \gtrsim 0.08 \left(\frac{10^{17}\text{ GeV}}{m_X}\right) \text{ eV} \tag{30}$$

which, actually, turns out to be independent on the specific form of the U_ν matrix as long as the 1-3 and 2-3 mixings therein are small (see the discussion above). With this at hand, any specific experimental upper limit on the absolute

---

[7]These, however, may not be that simple to get within potentially realistic unification chains, see Appendix C of Ref. [13].

[8]Given the structure of the seesaw formula in the current context (7) together with the tight constraints on the structure of the U_ν matrix we generally assume the hierarchy of the light neutrino mass eigenstates to be normal.

neutrino mass scale may be readily translated into a lower limit on m_X and, subsequently, the proton lifetime.

V. CONCLUSIONS AND OUTLOOK

The two-loop radiative RH neutrino mass generation mechanism originally identified by Witten in 1980s in the $SO(10)$ context finds a beautiful incarnation in the class of renormalizable flipped $SU(5)$ unified theories where, among other effects, it avoids the need for the 50-dimensional scalar representation. This, in turn, renders the simplest potentially realistic scenarios perhaps the most minimal (partially) unified gauge theories on the market, with strong implications for some of the key beyond-standard-model observables such as the absolute neutrino mass scale and proton decay.

In this work we have focused on a thorough evaluation of the relevant Feynman graphs in these scenarios paying particular attention to their analytic properties and the absolute size of the effect which turns out to be the key to the consistency of the scenario as a whole. It has been shown that there is no way to be consistent with the data with only one 5-dimensional scalar multiplet at play and, hence, the minimal potentially realistic setup must include two such irreps in the scalar sector (along with the 10-dimensional tensor).

As it turns out, such a minimal flipped $SU(5)$ model is subject to strong constraints on its allowed parameter space that lead to rather stringent limits on the absolute light neutrino mass scale as well as the BLNV two-body nucleon decays. A thorough numerical analysis of the corresponding correlations is deferred to a future study.

ACKNOWLEDGMENTS

APPENDIX A: THE INTERACTION LAGRANGIAN

The radiative generation of the RH neutrino masses involves only a small subset of the interactions associated with the full flipped $SU(5)$ Lagrangian. Working in the $SU(5) \otimes U(1)_X$ broken phase, we extract the required interactions from the kinetic terms and general Yukawa Lagrangian, Eq. (4), making use of FEYNRULES [28,29] and FEYNARTS [30,31] to verify that all terms and contributing diagrams are accounted for. As discussed in Sec. II, when the model contains only a single 5_H representation the relevant diagrams are found to be those in Fig. 1, arising from the interaction Lagrangian

$$\mathcal{L}_{\text{int}} \ni \frac{g_5^2}{2} \epsilon_{ijk} \epsilon^{\beta\alpha} V_G X_\alpha^{\mu i} X_{\mu\beta}^j \bar{D}^{\dagger k} + \frac{g_5}{\sqrt{2}} \epsilon_{ijk} X_{\mu\alpha}^i \bar{d}_{L_I}^{c\ j} \gamma^\mu Q_{L_I}^{k\alpha}$$

$$+ \frac{g_5}{\sqrt{2}} \epsilon^{\beta\alpha} X_{\mu\alpha}^i (\bar{Q}_{L_I})_{i\beta} \gamma^\mu \nu_{L_I}^c - 8 Y_{10}^{IJ} d_{L_I i}^{cT} C^{-1} \nu_{L_J}^c T^i$$

$$- 4 Y_{10}^{IJ} \epsilon_{ijk} \epsilon_{\alpha\beta} (Q_{L_I}^{i\beta})^T C^{-1} Q_{L_J}^{j\alpha} T^k + \text{H.c.} \quad (A1)$$

where i, j, k and α, β denote the $SU(3)_C$ and $SU(2)_L$ indices, respectively, and ϵ_{ijk} and $\epsilon_{\alpha\beta}$ are the relevant fully antisymmetric tensors with $\epsilon_{123} = -\epsilon^{12} = 1$. In this expression, $\bar{D}$ denotes the $(\bar{3}, 1, +\frac{1}{3})$ components of the scalar 10_H, T the $(3, 1, -\frac{1}{3})$ components of 5_H, Q_{L_I} the quark doublet $(3, 2, +\frac{1}{6}) \in 10_M$, $d_{L_I}^c$ the down-type quark singlet $(\bar{3}, 1, +\frac{1}{3}) \in 10_M$, and $\nu_{L_I}^c$ the $(1,1,0)$ components of 10_M. The charged vector bosons X_μ associated with the breaking of $SU(5) \otimes U(1)_X$ have SM quantum numbers $(3, \bar{2}, +\frac{1}{6})$. Following the breakdown of the $SU(5) \otimes U(1)_X$ symmetry due to the non-zero VEV V_G, the scalar states $\bar{D}$ and T mix to form the $SU(3)_C \otimes SU(2)_L \otimes U(1)_Y$ eigenstates $\Delta_{1,2}$, as described in Appendix B.

Let us note that in deriving the central formula Eq. (10), especially the overall factor of 3 therein, the color and isospin factors in Eq. (A1) play a crucial role. It is also worth noting that the exact cancellation of the UV divergences discussed in Sec. III, which relies on the extra factor of 2 in Eq. (11), emerges from the difference of the overall numerical factors in the last two terms in Eq. (A1).

After including an additional $5_H'$ to arrive at the minimal realistic model discussed in Section IV B, the interaction Lagrangian remains rather similar. The addition of Yukawa couplings involving $5_H'$ leads to the set of interaction terms (with color indices suppressed for simplicity)

$$\mathcal{L}_{\text{int}}^{\text{TH5M}} = \mathcal{L}_{\text{int}} - [8(Y_{10}')^{IJ} d_{L_I}^{cT} C^{-1} \nu_{L_J}^c T'$$

$$+ 4(Y_{10}')^{IJ} \epsilon_{\alpha\beta} (Q_{L_I}^\beta)^T C^{-1} Q_{L_J}^\alpha T' + \text{H.c.}], \quad (A2)$$

where T' denotes the additional $(3, 1, -\frac{1}{3})$ multiplet contained in $5_H'$, which mixes with the states $\bar{D}$ and T to yield a set of $SU(3)_C \otimes SU(2)_L \otimes U(1)_Y$ eigenstates $\Delta_{1,2,3}$.

For the sake of completeness and matching to the SM Yukawa couplings we also present the terms involving the doublet Higgs interactions here:

$$-\mathcal{L}_{\text{int}} \ni 8 Y_{10}^{IJ} \epsilon_{\gamma\delta} H^\delta d_{L_I}^{cT} C^{-1} Q_{L_J}^\gamma + Y_5^{IJ} H_\gamma^\dagger u_{L_J}^{cT} C^{-1} Q_{L_I}^\gamma$$

$$+ Y_{\bar{5}}^{IJ} H_\gamma^\dagger \nu_{L_I}^{cT} C^{-1} \ell_{L_J}^\gamma + Y_1^{IJ} \epsilon_{\gamma\delta} H^\gamma e_{L_J}^{cT} C^{-1} \ell_{L_I}^\delta$$

$$+ \text{H.c.}, \quad (A3)$$

where the SM Higgs doublet H consists of the components of 5_H transforming under the SM gauge group as $(1, 2, -\frac{1}{2})$, $u_{L_I}^c$ and ℓ_{L_I} are the components of $\bar{5}_M$ transforming as $(\bar{3}, 1, -\frac{2}{3})$ and $(1, 2, -\frac{1}{2})$ respectively, and $e_{L_I}^c$ denotes the single component of 1_M, transforming as $(1, 1, +1)$.

APPENDIX B: TRIPLET SCALAR SPECTRUM AND MIXING

1. Model with a single 5_H representation

The tree-level scalar potential in the model with a single 5_H may be written

$$
V = \frac{1}{2} m_{10}^2 \mathrm{Tr}(10_H^\dagger 10_H) + m_5^2 5_H^\dagger 5_H
$$

$$
+ \frac{1}{8}(\mu \epsilon_{ijklm} 10_H^{ij} 10_H^{kl} 5_H^m + \mathrm{H.c.})
$$

$$
+ \frac{1}{4}\lambda_1 [\mathrm{Tr}(10_H^\dagger 10_H)]^2 + \frac{1}{4}\lambda_2 \mathrm{Tr}(10_H^\dagger 10_H 10_H^\dagger 10_H)
$$

$$
+ \lambda_3 (5_H^\dagger 5_H)^2 + \frac{1}{2}\lambda_4 \mathrm{Tr}(10_H^\dagger 10_H)(5_H^\dagger 5_H)
$$

$$
+ \lambda_5 5_H^\dagger 10_H 10_H^\dagger 5_H. \tag{B1}
$$

The scalar basis is chosen such that the spontaneous breaking of $SU(5) \otimes U(1)_X$ and the subsequent electroweak symmetry breaking takes place via the nonzero VEVs

$$
\langle 10_H \rangle^{45} = -\langle 10_H \rangle^{54} = V_G, \qquad \langle 5_H \rangle^4 = v. \tag{B2}
$$

Requiring that this corresponds to a stationary point of the scalar potential yields the conditions

$$
V_G[m_{10}^2 + V_G^2(2\lambda_1 + \lambda_2) + v^2(\lambda_4 + \lambda_5)] = 0, \tag{B3}
$$

$$
v[m_5^2 + 2\lambda_3 v^2 + V_G^2(\lambda_4 + \lambda_5)] = 0, \tag{B4}
$$

which permit the parameters m_5^2, m_{10}^2 to be eliminated in favor of the VEVs.

After the breakdown of $SU(5) \otimes U(1)_X$ to $SU(3)_C \otimes SU(2)_L \otimes U(1)_Y$, the charged vector bosons X_μ associated with the broken generators acquire masses m_X given by Eq. (3). The scalar states T and $\bar{D}$ of relevance to the generation of the RH neutrino masses mix, with the mass matrix (in the basis $(\bar{D}^\dagger, T)$)

$$
M_\Delta^2 = \begin{pmatrix} -\lambda_2 V_G^2 & \mu V_G \\ \mu^* V_G & m_5^2 + \lambda_4 V_G^2 \end{pmatrix}, \tag{B5}
$$

where Eq. (B3) with $v = 0$ has been used to eliminate m_{10}^2. This is diagonalized by a unitary matrix U_Δ according to

$$
U_\Delta M_\Delta^2 U_\Delta^\dagger = \begin{pmatrix} m_{\Delta_1}^2 & 0 \\ 0 & m_{\Delta_2}^2 \end{pmatrix},
$$

with

$$
m_{\Delta_{1,2}}^2 = \frac{1}{2}\{m_5^2 + (\lambda_4 - \lambda_2)V_G^2
$$
$$
\mp \sqrt{[m_5^2 + (\lambda_2 + \lambda_4)V_G^2]^2 + 4|\mu|^2 V_G^2}\}, \tag{B6}
$$

which, in the electroweak vacuum, simplifies into

$$
m_{\Delta_{1,2}}^2 = \frac{V_G^2}{2}\left\{-(\lambda_2 + \lambda_5) \mp \sqrt{(\lambda_2 - \lambda_5)^2 + \frac{4|\mu|^2}{V_G^2}}\right\}. \tag{B7}
$$

The elements of the mixing matrix U_Δ read

$$
(U_\Delta)_{11} = \frac{\mu^* V_G}{\sqrt{|\mu|^2 V_G^2 + (m_{\Delta_1}^2 + \lambda_2 V_G^2)^2}},
$$

$$
(U_\Delta)_{12} = \frac{m_{\Delta_1}^2 + \lambda_2 V_G^2}{\sqrt{|\mu|^2 V_G^2 + (m_{\Delta_1}^2 + \lambda_2 V_G^2)^2}},
$$

$$
(U_\Delta)_{21} = \frac{\mu^* V_G}{\sqrt{|\mu|^2 V_G^2 + (m_{\Delta_2}^2 + \lambda_2 V_G^2)^2}},
$$

$$
(U_\Delta)_{22} = \frac{m_{\Delta_2}^2 + \lambda_2 V_G^2}{\sqrt{|\mu|^2 V_G^2 + (m_{\Delta_2}^2 + \lambda_2 V_G^2)^2}}. \tag{B8}
$$

2. Model with two 5_H representations

In the minimal realistic model with two 5_H representations, we take the tree-level scalar potential to be given by

$$
V = \frac{1}{2}m_{10}^2 \mathrm{Tr}(10_H^\dagger 10_H) + m_5^2 5_H^\dagger 5_H + m_{5'}^2 5_H'^\dagger 5_H' + \frac{1}{4}\lambda_1[\mathrm{Tr}(10_H^\dagger 10_H)]^2 + \frac{1}{4}\lambda_2 \mathrm{Tr}(10_H^\dagger 10_H 10_H^\dagger 10_H)
$$

$$
+ \lambda_3(5_H^\dagger 5_H)^2 + \tilde{\lambda}_3(5_H'^\dagger 5_H')^2 + \lambda_6(5_H^\dagger 5_H)(5_H'^\dagger 5_H') + \tilde{\lambda}_6(5_H^\dagger 5_H)(5_H'^\dagger 5_H') + \frac{1}{2}\lambda_4 5_H^\dagger 5_H \mathrm{Tr}(10_H^\dagger 10_H)
$$

$$
+ \frac{1}{2}\tilde{\lambda}_4 5_H'^\dagger 5_H' \mathrm{Tr}(10_H^\dagger 10_H) + \lambda_5 5_H^\dagger 10_H 10_H^\dagger 5_H + \tilde{\lambda}_5 5_H'^\dagger 10_H 10_H^\dagger 5_H'
$$

$$
+ \left[m_{12}^2 5_H^\dagger 5_H' + \frac{\mu}{8}\epsilon_{ijklm} 10_H^{ij} 10_H^{kl} 5_H^m + \frac{\mu'}{8}\epsilon_{ijklm} 10_H^{ij} 10_H^{kl} 5_H'^m + \eta_1(5_H^\dagger 5_H)(5_H^\dagger 5_H') + \eta_2(5_H^\dagger 5_H')^2\right.
$$

$$
\left. + \eta_3(5_H^\dagger 5_H)(5_H'^\dagger 5_H') + \frac{1}{2}\lambda_7 5_H^\dagger 5_H' \mathrm{Tr}(10_H^\dagger 10_H) + \lambda_8 5_H^\dagger 10_H 10_H^\dagger 5_H' + \mathrm{H.c.}\right]. \tag{B9}
$$

The field basis is again chosen such that the fields 10_H and 5_H acquire nonzero VEVs given by Eq. (B2), while

$$\langle 5'_H \rangle^4 = v'. \tag{B10}$$

The corresponding conditions that must hold for this to be a stationary point of the potential are

$$f_i = 0, i = 1, 2, 3, \tag{B11}$$

where

$$
\begin{aligned}
f_1 &= v_1 m_5^2 + v_2 m_{12}^2 + 3 v_1^2 v_2 \eta_1 + v_2^3 \eta_3 \\
&\quad + v_2 V_G^2 (\lambda_7 + \lambda_8) + 2 v_1^3 \lambda_3 + v_1 V_G^2 (\lambda_4 + \lambda_5) \\
&\quad + v_1 v_2^2 (\lambda_6 + \tilde{\lambda}_6 + 2\eta_2),
\end{aligned} \tag{B12}
$$

$$
\begin{aligned}
f_2 &= v_2 m_{5'}^2 + v_1 m_{12}^2 + v_1^3 \eta_1 + 3 v_1 v_2^2 \eta_3 \\
&\quad + v_1 V_G^2 (\lambda_7 + \lambda_8) + 2 v_2^3 \tilde{\lambda}_3 + v_2 V_G^2 (\tilde{\lambda}_4 + \tilde{\lambda}_5) \\
&\quad + v_1^2 v_2 (\lambda_6 + \tilde{\lambda}_6 + 2\eta_2),
\end{aligned} \tag{B13}
$$

$$
\begin{aligned}
f_3 &= V_G m_{10}^2 + V_G^3 (2\lambda_1 + \lambda_2) + v_1^2 V_G (\lambda_4 + \lambda_5) \\
&\quad + v_2^2 V_G (\tilde{\lambda}_4 + \tilde{\lambda}_5) + 2 v_1 v_2 V_G (\lambda_7 + \lambda_8).
\end{aligned} \tag{B14}
$$

In deriving the above, and in all expressions below, we restrict our attention to the case where all couplings are real.

In the $SU(3)_C \otimes SU(2)_L \otimes U(1)_Y$ symmetric phase, i.e., for $V_G \neq 0$, $v = v' = 0$, the set of scalar color triplets that mix is extended to include the color triplet T' associated with $5'_H$. The 3×3 mass matrix, in the basis $(\bar{D}^\dagger, T, T')$, reads

$$
M_\Delta^2 = \begin{pmatrix} -\lambda_2 V_G^2 & \mu V_G & \mu' V_G \\ \mu V_G & m_5^2 + \lambda_4 V_G^2 & m_{12}^2 + \lambda_7 V_G^2 \\ \mu' V_G & m_{12}^2 + \lambda_7 V_G^2 & m_{5'}^2 + \tilde{\lambda}_4 V_G^2 \end{pmatrix}, \tag{B15}
$$

where Eq. (B14) with $v = v' = 0$ has been used to eliminate the dependence on m_{10}^2. The resulting mass eigenstates $(\Delta_1, \Delta_2, \Delta_3)$ are obtained through the rotation

$$
\begin{pmatrix} \Delta_1 \\ \Delta_2 \\ \Delta_3 \end{pmatrix} = U_\Delta \begin{pmatrix} \bar{D}^\dagger \\ T \\ T' \end{pmatrix}, \tag{B16}
$$

where the unitary matrix U_Δ diagonalizes M_Δ^2 according to

$$
U_\Delta M_\Delta^2 U_\Delta^\dagger = \mathrm{diag}(m_{\Delta_1}^2, m_{\Delta_2}^2, m_{\Delta_3}^2). \tag{B17}
$$

APPENDIX C: RADIATIVE FERMION MASS GENERATION

In general, the physical mass of a single spin-1/2 fermion is obtained as the value of m for which

$$(\not{k} + m)\Gamma^{(2)}(k) = 0 \quad \forall \ k \text{ such that } k^2 = m^2, \tag{C1}$$

where $\Gamma^{(2)}(k)$ is the renormalized two-point 1PI Green's function,

$$\Gamma^{(2)}(k) = Z(k)\not{k} - \Sigma(0). \tag{C2}$$

In this expression, $Z(k)$ corresponds to the wave function renormalization and $\Sigma(0)$ is the zero incoming momentum contribution to the appropriate sum of Feynman diagrams. Taken together, Eq. (C1) and Eq. (C2) imply that

$$mZ(m^2) = \Sigma(0), \tag{C3}$$

which generally amounts to a transcendental equation to be solved for the physical mass m. An expression for m may be obtained perturbatively by writing $Z(m^2) = 1 + \Delta Z(m^2)$, $\Sigma(0) = m_0 + \Delta m_0$, where the first and second term in each expression correspond to the tree-level and loop corrections to each quantity, respectively. One finds the result

$$m = m_0 + [\Delta m_0 - m_0 \Delta Z(m_0^2)] + \dots, \tag{C4}$$

where we show only the leading part of the higher-order contribution. Therefore, in the general case with $m_0 \neq 0$, a calculation of the leading higher-order contribution to the physical mass would require the evaluation of the loop corrections to both $\Sigma(0)$ and $Z(k^2)$.

However, for the case studied in this article in which the RH neutrinos are massless at tree-level, Eq. (C4) reads simply $m = \Delta m_0 = \Sigma(0)$ at leading order.

APPENDIX D: EVALUATION OF THE TWO LOOP FEYNMAN INTEGRALS

1. Veltman-Van der Bij brackets

Remarkably enough, there is an entire industry concerning the evaluation methods for the zero-external-momentum two-point 1PI graphs, see, e.g., Ref. [22] or Ref. [27] and references therein.

The principal object in these methods are the so-called Veltman-Van der Bij brackets. As the original paper uses an Euclidean metric and a different choice of dimensional regularization parameter ϵ, we give here all of the relevant expressions in our particular convention, i.e., in Minkowski metric $g = \mathrm{diag}(1, -1, -1, -1)$ and with the number of spacetime dimensions equal to $D = 4 - 2\epsilon$.

We introduce the brackets in the following way

$$\{M_{11}, M_{12}, \ldots; M_{21}, \ldots; M_{31}, \ldots\} = \int \frac{d^4 p}{(2\pi)^4} \int \frac{d^4 q}{(2\pi)^4} \frac{1}{(p^2 - M_{11}^2)(p^2 - M_{12}^2)\ldots} \frac{1}{(q^2 - M_{21}^2)\ldots} \frac{1}{[(p+q)^2 - M_{31}^2]\ldots},$$

(D1)

$$\{M_{11}, M_{12}, \ldots\} = \int \frac{d^4 p}{(2\pi)^4} \frac{1}{(p^2 - M_{11}^2)(p^2 - M_{12}^2)\ldots},$$

(D2)

$$\{M_{11}, \ldots; M_{21}, \ldots; M_{31}, \ldots\}[A(p,q)] = \int \frac{d^4 p}{(2\pi)^4} \int \frac{d^4 q}{(2\pi)^4} \frac{1}{(p^2 - M_{11}^2)\ldots} \frac{1}{(q^2 - M_{21}^2)\ldots} \frac{1}{[(p+q)^2 - M_{31}^2]\ldots} A(p,q). \quad \text{(D3)}$$

With the last expression we have introduced a shorthand notation that simplifies the form of this Appendix.

Note that the brackets are invariant under the exchange of positions of the individual groups of components, which can be obtained by the change of variables $(p \leftrightarrow q)$ and $(p + q \rightarrow p, -q \rightarrow q)$.

By a partial cancellation of fractions we can derive various reduction formulae of the type

$$\{M_A, m_a; M_B, m_b; M_C\}[p^2]$$
$$= \{M_A; M_B, m_b; M_C\} + m_a^2 \{M_A, m_a; M_B, m_b; M_C\}.$$

(D4)

A similar trick using $p^2 - M_B^2 - (p^2 - M_A^2) = M_A^2 - M_B^2$ can be used for a simplification of brackets of the type[9]

$$\{M_A, M_B; \alpha; \beta\} = \frac{1}{M_A^2 - M_B^2} (\{M_A; \alpha; \beta\} - \{M_B; \alpha; \beta\}).$$

(D6)

It is also possible to show that

$$\{M_A; M_B; M_C\}[(p+q)^2]$$
$$= \{M_A\}\{M_B\} + M_C^2 \{M_A; M_B; M_C\}.$$

(D7)

Using all of these methods we can express the relevant two-loop integrals in terms of simple brackets $\{M_A; M_B; M_C\}$. It is of use to rewrite them further into double brackets

$$\{2M_A; M_B; M_C\} \equiv \{M_A, M_A; M_B; M_C\}, \quad \text{(D8)}$$

which are dimensionless (cf. Ref. [22]). The operation transcribing simple brackets into double brackets is 't Hooft's p-operation [32]. In our notation it reads

$$\{M_A; M_B; M_C\} = \frac{1}{D-3} (M_A^2 \{2M_A; M_B; M_C\}$$
$$+ M_B^2 \{2M_B; M_C; M_A\}$$
$$+ M_C^2 \{2M_C; M_A; M_B\}).$$

(D9)

2. Topology 1

Topology 1 of Fig. 1 leads to the kinematic form (i.e., neglecting the specific form of the vertices) of the integral given in Eq. (12). By using D-dimensional gamma matrix gymnastics, it can be simplified into

$$\Sigma_1^P(0) = -\{m_X, 0; m_X, 0; m_{\Delta_i}\} \left[(D-4)\slashed{q}\slashed{p} + 4p \cdot q \right.$$
$$\left. - \frac{p^2 + q^2}{m_X^2} \slashed{p}\slashed{q} + \frac{p^2 q^2}{m_X^4} p \cdot q \right].$$

(D10)

The slashed product can be rewritten into $\slashed{p}\slashed{q} = p \cdot q - i p^\mu \sigma_{\mu\nu} q^\nu$. After performing the p integration the second term would have to be of the form $iq^\mu \sigma_{\mu\nu} q^\nu$ and, due to the antisymmetry of $\sigma_{\mu\nu}$, such a term will not contribute. After the operations given above, we obtain

$$\Sigma_1^P(0) = -\frac{m_{\Delta_i}^2}{2m_X^4} \{0; 0; m_{\Delta_i}\} - (D-1) \left(\frac{1}{2m_X^4} A_0(m_X^2)^2 \right.$$
$$\left. + \frac{m_{\Delta_i}^2}{2} \{m_X, 0; m_X, 0; m_{\Delta_i}\} - \{m_X, 0; m_X; m_{\Delta_i}\} \right).$$

(D11)

This may be rewritten in terms of the simple brackets using relations similar to those in Eq. (D6).

─────────

[9]Note that this simplification relates together the Passarino-Veltman integrals A_0 and B_0,

$$B_0(0, 0, M_A^2) = \{M_A, 0\} = \frac{1}{M_A^2} \{M_A\} = \frac{1}{M_A^2} A_0(M_A^2). \quad \text{(D5)}$$

3. Topology 2

Neglecting the specific form of the vertices, Topology 2 of Fig. 1 leads to the second integral in Eq. (12). It can be simplified into (again making use of the antisymmetry of $\sigma_{\mu\nu}$)

$$\Sigma_2^P(0) = -\{m_X, 0; m_{\Delta_i}, 0; m_X\}\left[(2-D)p\cdot q\right.$$

$$-\frac{2p^2q^2}{m_X^2} - \frac{2p^2+q^2}{m_X^2}p\cdot q + \frac{p^4q^2}{m_X^4}$$

$$\left. +\frac{p^2(q^2+p^2)}{m_X^4}p\cdot q + \frac{p^2}{m_X^4}(p\cdot q)^2\right]. \quad (D12)$$

The result after simplification reads

$$\Sigma_2^P(0) = \frac{2-D}{2}\{0; m_{\Delta_i}, 0; m_X\} + \frac{3-D}{2}\{m_X, 0; m_{\Delta_i}; m_X\}$$

$$+\frac{m_{\Delta_i}^2}{4m_X^4}(2\{m_X; 0; m_{\Delta_i}\} - \{m_X; m_X; m_{\Delta_i}\})$$

$$+\frac{D-2}{2m_{\Delta_i}^2 m_X^2}A_0(m_X^2)A_0(m_{\Delta_i}^2) - \frac{1}{4m_X^4}A_0(m_X^2)^2. \tag{D13}$$

4. Integrals

For the reader's convenience, we list here the results of the integrals appearing in the expressions in our convention. As integrals $A_0(M_A^2)$ appear in the results in the second power, we need to evaluate also the term linear in ϵ. This gives

$$A_0(M_A^2) = Q^{4-D}\int \frac{d^D p}{(2\pi)^D}\frac{1}{p^2-M_A^2}$$

$$= -i\frac{M_A^2}{(4\pi)^2}\left[-\frac{1}{\epsilon} + L_A - \frac{\epsilon}{2}\left(L_A^2 + 1 + \frac{\pi^2}{6}\right)\right]$$

$$+ O(\epsilon^2), \tag{D14}$$

where

$$L_A = \log\frac{M_A^2}{Q^2} - \log 4\pi + \gamma - 1, \tag{D15}$$

with Q being the renormalization scale and γ the Euler-Mascheroni constant.

As was already stated, all of the simple brackets can be obtained from the double brackets using Eq. (D9). Therefore, we give here the result only for them. It reads

$$\{2M; M_a; M_b\} = \frac{1}{(4\pi)^4}(S(M) - f(a,b)) + O(\epsilon), \quad (D16)$$

where

$$S(M) = -\frac{1}{2\epsilon^2} + \frac{1}{\epsilon}\left(L + \frac{1}{2}\right) - \left(L^2 + L + \frac{1}{2} + \frac{\pi^2}{12}\right), \tag{D17}$$

$$a = \frac{M_a^2}{M^2}, \qquad b = \frac{M_b^2}{M^2}, \tag{D18}$$

and the function $f(a,b)$ is given by

$$f(a,b) = -\frac{1}{2}\log a \log b + \frac{1-a-b}{2\sqrt{q}}\left[\mathrm{Li}_2\left(-\frac{x_2}{y_1}\right) + \mathrm{Li}_2\left(-\frac{y_2}{x_1}\right) - \mathrm{Li}_2\left(-\frac{x_1}{y_2}\right) - \mathrm{Li}_2\left(-\frac{y_1}{x_2}\right)\right.$$

$$\left. + \mathrm{Li}_2\left(\frac{b-a}{x_2}\right) + \mathrm{Li}_2\left(\frac{a-b}{y_2}\right) - \mathrm{Li}_2\left(\frac{b-a}{x_1}\right) - \mathrm{Li}_2\left(\frac{a-b}{y_1}\right)\right], \tag{D19}$$

$$f(b,b) = -\frac{(2b-1)\left(2\mathrm{Li}_2\left(\frac{\sqrt{1-4b}-1}{\sqrt{1-4b}+1}\right) + \frac{\pi^2}{6} + \frac{1}{2}\log^2\left(-\frac{\sqrt{1-4b}-1}{\sqrt{1-4b}+1}\right)\right)}{\sqrt{1-4b}} - \frac{1}{2}\log^2(b). \tag{D20}$$

In Eq. (D19) and Eq. (D20) the quantities q, $x_{1,2}$, and $y_{1,2}$ are defined by

$$q \equiv 1 - 2(a+b) + (a-b)^2, \tag{D21}$$

$$x_{1,2} \equiv \frac{1}{2}(1 + b - a \pm \sqrt{q}), \tag{D22}$$

$$y_{1,2} \equiv \frac{1}{2}(1 + a - b \pm \sqrt{q}). \tag{D23}$$

In addition to Eq. (D20) giving the value of $f(a,b)$ when $a=b$, it is helpful to note the other special cases

$$f(0,0) = \frac{\pi^2}{6}, \tag{D24}$$

$$f(0,b) = \mathrm{Li}_2(1-b), \tag{D25}$$

$$f(0,b^{-1}) = -\frac{1}{2}\log^2 b - f(0,b). \tag{D26}$$

5. The kinematic structure of the self-energies

Rewriting Eq. (D11) and Eq. (D13) yields the expressions in terms of double brackets,

$$\Sigma_1^P(0) = -\frac{1}{D-3}\frac{m_{\Delta_i}^4}{2m_X^4}\{2m_{\Delta_i};0;0\} - \frac{D-1}{2m_X^4}A_0(m_X^2)^2 + \frac{D-1}{D-3}(2\{2m_X;m_X;m_{\Delta_i}\} - \{2m_X;0;m_{\Delta_i}\})$$

$$+ \frac{D-1}{D-3}\frac{m_{\Delta_i}^4}{2m_X^4}(2\{2m_{\Delta_i};m_X;0\} - \{2m_{\Delta_i};m_X;m_X\} - \{2m_{\Delta_i};0;0\})$$

$$+ \frac{D-1}{D-3}\frac{m_{\Delta_i}^2}{m_X^2}(\{2m_X;0;m_{\Delta_i}\} - \{2m_X;m_X;m_{\Delta_i}\} + \{2m_{\Delta_i};m_X;m_X\} - \{2m_{\Delta_i};m_X;0\}), \tag{D27}$$

$$\Sigma_2^P(0) = \frac{D-2}{2m_{\Delta_i}^2 m_X^2}A_0(m_X^2)A_0(m_{\Delta_i}^2) - \frac{1}{4m_X^4}A_0(m_X^2)^2 + \frac{D-2}{D-3}\frac{m_X^2}{2m_{\Delta_i}^2}(\{2m_X;0;0\} - \{2m_X;0;m_{\Delta_i}\})$$

$$+ \frac{m_{\Delta_i}^2}{2m_X^2}(\{2m_{\Delta_i};m_X;0\} - \{2m_{\Delta_i};m_X;m_X\}) + \frac{1}{D-3}\frac{m_{\Delta_i}^2}{2m_X^2}(\{2m_X;0;m_{\Delta_i}\} - \{2m_X;m_X;m_{\Delta_i}\})$$

$$- \frac{D-2}{2(D-3)}\{2m_{\Delta_i};m_X;0\} - \frac{1}{2}(2\{2m_X;m_X;m_{\Delta_i}\} - \{2m_X;0;m_{\Delta_i}\})$$

$$+ \frac{1}{D-3}\frac{m_{\Delta_i}^4}{4m_X^4}(2\{2m_{\Delta_i};m_X;0\} - \{2m_{\Delta_i};m_X;m_X\}). \tag{D28}$$

Using the explicit expression for the double brackets, Eq. (D16), $\Sigma_1^P(0)$ and $\Sigma_2^P(0)$ are then finally found to be given by (where $s_i = \frac{m_{\Delta_i}^2}{m_X^2}$ as above)

$$(4\pi)^4\Sigma(0)_1^P = -\frac{3}{2\epsilon} + 3L_X - 2 + \frac{s_i^2}{2}\left[\frac{1}{2\epsilon^2} - \frac{1}{\epsilon}\left(L_{\Delta_i} - \frac{1}{2}\right) + \left(L_{\Delta_i}^2 - L_{\Delta_i} + \frac{3}{2} + \frac{\pi^2}{12}\right)\right]$$

$$+ 3(f(0,s_i) - 2f(1,s_i)) + \frac{3}{2}s_i^2[f(s_i^{-1},s_i^{-1}) - 2f(0,s_i^{-1})]$$

$$+ 3s_i[f(1,s_i) - f(0,s) - f(s_i^{-1},s_i^{-1}) + f(0,s_i^{-1})] + 2s_i^2 f(0,0), \tag{D29}$$

$$(4\pi)^4\Sigma(0)_2^P = \frac{3}{4\epsilon} - \frac{1}{2}[L_X + 2L_{\Delta_i} - (L_{\Delta_i} - L_X)^2 - 1] - \frac{s_i^2}{4}\left[\frac{1}{2\epsilon^2} - \frac{1}{\epsilon}\left(L_{\Delta_i} - \frac{1}{2}\right) + \left(L_{\Delta_i}^2 - L_{\Delta_i} + \frac{3}{2} + \frac{\pi^2}{12}\right)\right]$$

$$- s_i^{-1}[f(0,0) - f(0,s_i)] + f(0,s_i^{-1}) + f(1,s_i) - \frac{1}{2}f(0,s_i)$$

$$- \frac{s_i}{2}[f(s_i^{-1},0) - f(s_i^{-1},s_i^{-1}) + f(0,s_i) - f(1,s_i)] - \frac{s_i^2}{4}[2f(0,s_i^{-1}) - f(s_i^{-1},s_i^{-1})]. \tag{D30}$$

Note that the individual diagrams are UV divergent, with the divergent terms given by Eqs. (14) and (15). However, as noted in Sec. III, their combination appearing in Eq. (11) yielding the total contribution to the RH neutrino mass matrix is finite and compact,

$$I_3(s) = 1 + 2\log s + s(1 - 2s)\log^2 s + 2(s^{-1} - 1)[f(0,0)(1 + s + s^2) + 2sf(1,s)$$

$$+ f(0,s)(1 + s)(1 + 2s) + s^2 f(s^{-1}, s^{-1})]. \tag{D31}$$

[1] A. De Rújula, H. Georgi, and S. L. Glashow, Phys. Rev. Lett. **45**, 413 (1980).
[2] S. M. Barr, Phys. Lett. **112B**, 219 (1982).
[3] J. P. Derendinger, J. E. Kim, and D. V. Nanopoulos, Phys. Lett. B **139**, 170 (1984).
[4] J. Ellis, T. E. Gonzalo, J. Harz, and W.-C. Huang, J. Cosmol. Astropart. Phys. 03 (2015) 039.
[5] M. Cannoni, J. Ellis, M. E. Gómez, S. Lola, and R. R. de Austri, J. Cosmol. Astropart. Phys. 03 (2016) 041.
[6] H. Sonmez, Phys. Rev. D **93**, 125002 (2016).
[7] H.-Y. Chen, I. Gogoladze, S. Hu, T. Li, and L. Wu, Eur. Phys. J. C **78**, 26 (2018).
[8] H. Georgi and S. L. Glashow, Phys. Rev. Lett. **32**, 438 (1974).
[9] S. Bertolini, L. Di Luzio, and M. Malinský, Phys. Rev. D **81**, 035015 (2010).
[10] S. Bertolini, L. Di Luzio, and M. Malinský, Phys. Rev. D **85**, 095014 (2012).
[11] C. R. Das, C. D. Froggatt, L. V. Laperashvili, and H. B. Nielsen, Mod. Phys. Lett. A **21**, 1151 (2006).
[12] G. K. Leontaris and J. D. Vergados, Phys. Lett. B **258**, 111 (1991).
[13] C. A. Rodríguez, H. Kolešová, and M. Malinský, Phys. Rev. D **89**, 055003 (2014).
[14] E. Witten, Phys. Lett. **91B**, 81 (1980).
[15] A. Osipowicz et al., arXiv:hep-ex/0109033.
[16] C.-K. Chua, X.-G. He, and W.-Y. P. Hwang, Phys. Lett. B **479**, 224 (2000).
[17] U. Mahanta, Phys. Rev. D **62**, 073009 (2000).
[18] D. A. Sierra, M. Hirsch, and S. G. Kovalenko, Phys. Rev. D **77**, 055011 (2008).
[19] I. Doršner, S. Fajfer, and N. Košnik, Eur. Phys. J. C **77**, 417 (2017).
[20] K. Abe et al., Phys. Rev. D **96**, 012003 (2017).
[21] P. Nath and P. F. Pérez, Phys. Rep. **441**, 191 (2007).
[22] J. van der Bij and M. J. G. Veltman, Nucl. Phys. **B231**, 205 (1984).
[23] D. J. Broadhurst, Z. Phys. C **47**, 115 (1990).
[24] C. Ford and D. R. T. Jones, Phys. Lett. B **274**, 409 (1992); **285**, 398(E) (1992).
[25] C. Ford, I. Jack, and D. R. T. Jones, Nucl. Phys. **B387**, 373 (1992); **B504**, 551 (1997).
[26] A. I. Davydychev and J. B. Tausk, Nucl. Phys. **B397**, 123 (1993).
[27] D. A. Sierra, A. Degee, L. Dorame, and M. Hirsch, J. High Energy Phys. 03 (2015) 040.
[28] N. D. Christensen and C. Duhr, Comput. Phys. Commun. **180**, 1614 (2009).
[29] A. Alloul, N. D. Christensen, C. Degrande, C. Duhr, and B. Fuks, Comput. Phys. Commun. **185**, 2250 (2014).
[30] J. Küblbeck, M. Böhm, and A. Denner, Comput. Phys. Commun. **60**, 165 (1990).
[31] T. Hahn, Comput. Phys. Commun. **140**, 418 (2001).
[32] G. 't Hooft and M. J. G. Veltman, Nucl. Phys. **B44**, 189 (1972).